

Thiol Modification of Cysteine 327 in the Eighth Transmembrane Domain of the Light Subunit xCT of the Heteromeric Cystine/Glutamate Antiporter Suggests Close Proximity to the Substrate Binding Site/Permeation Pathway*

Received for publication, September 5, 2003, and in revised form, January 8, 2004
Published, JBC Papers in Press, January 13, 2004, DOI 10.1074/jbc.M309866200

Maite Jiménez-Vidal^{‡§¶}, Emma Gasol^{‡||}, Antonio Zorzano[‡], Virginia Nunes[§], Manuel Palacín^{‡***‡‡}, and Josep Chillarón^{‡***§§}

From the [‡]Department of Biochemistry and Molecular Biology, Faculty of Biology, and the Barcelona Science Park, University of Barcelona, E-08028 Barcelona, Spain and the [§]Medical and Molecular Genetics Center, Institut de Recerca Oncològica, L'Hospitalet de Llobregat, E-08028 Barcelona, Spain

We measured sensitivity to thiol modification of the heteromeric glutamate/cystine transporter 4F2hc-xCT expressed in *Xenopus* oocytes. *p*-Chloromercuribenzoate (pCMB) and *p*-chloromercuribenzenesulfonate (pCMBS) rapidly blocked transport activity. Cys³²⁷, located in the middle of the eighth transmembrane domain of the light subunit (xCT), was found to be the main target of inactivation. Cysteine, an impermeant reducing reagent, reversed pCMB and pCMBS effects only when applied from the extracellular medium. L-Glutamate and L-cystine, but not L-arginine, protected from the inactivation with an IC₅₀ similar to the *K_m*. Protection was not temperature-dependent, suggesting that it did not depend on large substrate-induced conformational changes. Mutation of Cys³²⁷ to Ala and Ser slightly modified the *K_m* and a C327L mutant abolished transport function without compromising transporter expression at the plasma membrane. The results indicate that Cys³²⁷ is a functionally important residue accessible to the aqueous extracellular environment and is structurally linked to the permeation pathway and/or the substrate binding site.

Heteromeric amino acid transporters (HATs)¹ are composed of a heavy subunit and a light subunit (LSHAT) linked by a

* This study was supported in part by the Spanish Ministry of Science and Technology (PM99-017-CO-01/02 and SAF2003-08940 to M. P. and V. N.), the Institut de Salut Carlos III (Networks C3/08P to M. P., G03/054 to M. P. and V. N., and C03/07 to V. N.), and the Comissionat per a Universitats i Recerca (to M. P.). The costs of publication of this article were defrayed in part by the payment of page charges. This article must therefore be hereby marked "advertisement" in accordance with 18 U.S.C. Section 1734 solely to indicate this fact.

[†] Supported by BIOMED Grant BMH4 CT98-3514.

^{||} Recipient of a pre-doctoral fellowship from the Spanish Ministry of Education and Culture.

** These authors share lead authorship.

^{‡‡} To whom correspondence may be addressed: Barcelona Science Park, Josep Samitier 1–5, 08028 Barcelona, Spain. Tel.: 34-934034617; Fax 34-934021559; E-mail: mpalacin@bio.ub.es.

^{§§} A researcher from the Programa Ramón y Cajal of the Spanish Ministry of Science and Technology. To whom correspondence may be addressed: Dept. of Biochemistry and Molecular Biology, New Bldg., Faculty of Biology, University of Barcelona, Av. Diagonal 645, E-08028 Barcelona, Spain. Tel.: 34-934034700; Fax: 34-934034717; E-mail: chillaron@worldonline.es.

¹ The abbreviations used are: HAT, heteromeric amino acid transporter; LSHAT, HAT light subunit; pCMB, *p*-chloromercuribenzoate; pCMBS, *p*-chloromercuribenzenesulfonate; NEM, *N*-ethylmaleimide; MTS, methanethiosulfonate; APC, amino acid/polyamine/organic cation; APA, basic amino acid/polyamine antiporter; GABP, *E. coli* γ -aminobutyric acid permease.

conserved disulfide bridge (1, 2). The heavy subunit is important for trafficking of the heterodimer to the plasma membrane, whereas the light subunit confers transport function and specificity (3, 4). Two heavy subunits are known, 4F2hc and rBAT (1, 2). The light subunit xCT bound to 4F2hc elicits sodium-independent transport of anionic L-cystine and L-glutamate by a 1:1 obligatory exchange (system x_c⁻) (5, 6). xCT is expressed in most cell lines, in activated macrophages, and in the brain (5, 7). System x_c⁻ functions physiologically for cystine uptake and glutamate efflux because of the low and high intracellular concentrations of cystine and glutamate, respectively. Cytosolic cystine concentrations are kept very low because of its rapid reduction to cysteine, the main source for the synthesis of intracellular glutathione. Indeed, transport of cystine and its intracellular reduction to cysteine are the rate-limiting steps in glutathione biosynthesis (5, 8). This is consistent with the known regulation of xCT; its mRNA and x_c⁻ activity are induced by lipopolysaccharide in macrophages, and this induction is modulated by the ambient oxygen concentration (*i.e.* hypoxia decreases xCT expression and activity) (9). Moreover, the xCT gene carries an electrophil-response element that may mediate some of these effects (10). The authors concluded that xCT provides an antioxidant defense for these cells, especially in regions of inflammation. In the brain, the localization of xCT suggests that it contributes to the maintenance of the redox state in the cerebrospinal fluid (7).

Little is known about the structure-function relationships of the HAT family. Reconstitution studies with the b^{0,+}AT light subunit have shown that the rBAT heavy subunit is not necessary for the basic transport function (4). The relevant functional determinants should lie on the LSHATs. The topology of LSHATs has not been tested experimentally but is believed to adopt the classic model of 12-transmembrane domains. An approximation to the substrate binding site of LAT1 has been proposed based on substrate specificity and semi-empirical computational analysis (11, 12). Recently, Boado *et al.* (13) reported a naturally occurring interspecific change (W234L) that slightly modified LAT1 *K_m*. Finally, the y⁺LAT1 L334R mutant found in lysinuric protein-intolerant patients inactivates transport as does the cystinuria mutation, A354T in b^{0,+}AT (4, 14).

Here we report that Cys³²⁷ in transmembrane domain 8 of the xCT light subunit is the target for transport inactivation caused by organic mercury compounds. We provide evidence that this residue may be closely linked to the substrate permeation pathway. To our knowledge, this is the first report to provide significant experimental insight into the structure-

function of the LSHATs as well as a framework for a systematic study (15) of this family.

EXPERIMENTAL PROCEDURES

Site-directed Mutagenesis—Construction of human 4F2hc Cysless has been described elsewhere (16). The human xCT in pNKS2 was used as the template for site-directed mutagenesis (QuikChange™, Stratagene). A Cysless xCT was engineered by replacing the seven endogenous cysteine residues with serine. The mutated regions were excised by digestion with the appropriate restriction enzymes and subcloned back into the original plasmid. At position 327, cysteine was also mutated to Ala, Leu, and Thr, and the mutated region was then subcloned into N-terminally Myc-tagged human xCT (in pNKS2) with the appropriate restriction enzymes. Cysteine 327 was reintroduced into Cysless xCT by restriction enzyme digestion and subcloning into the Cysless construct. Mutations were confirmed by DNA sequencing. Sequencing was performed on both strands with a d-Rhodamine dye Terminator Cycle Sequencing Ready Reaction Kit (PerkinElmer Life Sciences). The sequence reactions were analyzed with an Abi Prism 377 DNA sequencer.

cRNA Preparation and Microinjection into *Xenopus* Oocytes—Synthesis of human wild type and Cysless 4F2hc cRNAs has been described elsewhere (16). *In vitro* synthesis of human xCT construct cRNAs was conducted with the NotI-linearized plasmid template using the protocol provided by Ambion (mMessage mMachine, Ambion, Austin, TX). The quality and the amount of transcribed RNA were checked by gel inspection and 260 nm absorbance before microinjection into *Xenopus* oocytes. The procedure for *Xenopus* oocyte isolation and the microinjection technique are described elsewhere (17). Defolliculated stage VI *Xenopus laevis* oocytes were injected with 50 nl of human 4F2hc and human xCT constructs alone or in combination (10 ng/oocyte).

Transport Measurement—Influx rates of L-[³H]glutamate (American Radiolabeled Chemicals) and L-[³⁵S]cystine (Amersham Biosciences) were measured at 1 μCi/μl in 100 mM choline-Cl medium 2 or 3 days after injection and under linear conditions as described elsewhere (6). Amino acid transport rates obtained with oocytes injected with water (50 nl) were similar to those of noninjected oocytes (data not shown). Results for transport experiments are given as mean ± S.E. for 6–8 individual oocytes. For the determination of the kinetic parameters of the different human xCT Cys³²⁷ mutants, the oocytes were incubated with different concentrations of L-glutamate (5, 10, 25, 50, 100, 250, 500 μM, 1 and 2 mM). V_{max} and K_m values were derived by the Michaelis-Menten equation using GraphPad Prism. Each experiment was performed at least twice on different batches of oocytes. Nonradioactive amino acids and chemicals were purchased from Sigma.

Determination of the Effect of Sulfhydryl Reagents—Oocytes were incubated for 5 min at room temperature with choline-Cl medium containing 1 mM *p*-chloromercuribenzoate (pCMB), 1 mM *p*-chloromercuribenzenesulfonate (pCMBS), 5 mM *N*-ethylmaleimide (NEM), 1 mM [2-(trimethylammonium)ethyl] methanethiosulfonate (MTSET), 2.5 mM 2-aminoethyl methanethiosulfonate (MTSEA), 10 mM 2-sulfonatoethyl methanethiosulfonate (MTSES), 1 mM [4-(*N*-maleimido)benzyl] trimethylammonium (MBTA), 1 mM iodoacetamide, or 1 mM mersalyl acid and washed three times in choline-Cl medium. Subsequently transport of L-[³H]glutamate or L-[³⁵S]cystine was assayed. To test whether methanethiosulfonate (MTS) reagents, iodoacetamide, NEM, and mersalyl acid reached the human xCT 327 cysteine, a second incubation was performed with 1 mM pCMB for 5 min before uptake measurement. For the protection assays, 2 mM L-glutamate, 2 mM L-arginine, or 300 μM L-cystine was added to the choline-Cl medium with pCMB or pCMBS and incubated at room temperature for 10 min (if not otherwise indicated on the figure). For some experiments different concentrations of unlabeled L-glutamate (5, 10, 25, 50, 100, 250, or 500 μM or 1 or 2 mM) or L-cystine (6, 15, 30, 60, 90, 150, or 300 μM) were included along with 50 μM pCMB during the 10-min preincubation step. For protection experiments at 4 °C, the preincubation step was done at 4 °C at the times indicated on Fig. 4. Then, oocytes were washed three times at room temperature in choline-Cl medium to remove unbound sulfhydryl reagent and amino acids. Transport was then measured as described above. In reactivation experiments, following incubation with the sulfhydryl reagents, either 10 mM free cysteine or 5 mM β-mercaptoethanol was added to the medium for 5, 10, and 20 min. At the end of the incubation, the oocytes were washed three times in choline-Cl medium, and transport was then measured as described above. The MTS reagents and pCMBS were purchased from Toronto Research Chemicals, Inc. pCMB, mersalyl acid, iodoacetamide, and NEM were purchased from Sigma. Each of the sulfhydryl reagents was dissolved as a 1 M

stock solution (MTS reagents, NEM, and iodoacetamide) or as a 100 mM stock solution (pCMB and pCMBS) in Me₂SO. After dilution in choline-Cl medium to the final concentration, the reagents were used immediately.

Immunofluorescence Microscopy—Groups of five oocytes were prepared for immunofluorescence 3 days after injection with 10 ng of human 4F2hc, *N*-myc-human xCT wild type, or Cys³²⁷ mutant cRNA/oocyte, alone or in combination. Oocytes were placed in 500-μm³ cryomolds (Tissue-Tek, Miles, Elkhart, IN) and then sliced, fixed, and permeabilized as described elsewhere (16). Slices were incubated with monoclonal antibody 9E10 anti-Myc (ATCC, Manassas, VA), diluted 1:500 in 10% phosphate-buffered saline, at room temperature for 1 h. Slices were washed three times in phosphate-buffered saline, incubated with 7.5 μg/ml Texas Red-conjugated goat anti-mouse (Molecular Probes, Leiden, The Netherlands) at room temperature for 1 h, washed three times in phosphate-buffered saline, and mounted in Immunofluore (ICN, Madrid, Spain).

Data Analysis—Nonlinear regression fits of experimental and calculated data were performed with GraphPad Prism. The half-life times ($t_{1/2}$) and IC₅₀ values were determined by plotting the fraction of uptake remaining ($F = \text{uptake after/uptake before}$) as a function of the concentration or time of incubation of the reagent and then fitted to a nonlinear regression equation for one-phase exponential decay ($F = F_{max} \times e^{(-K_c \times t)} + F_{min}$ or $F = F_{max} \times e^{(-K_r \times c)} + F_{min}$) where t is the incubation time in seconds, c is the concentration of reagent, and K_c and K_r are the pseudo first-order rate constants (when concentration or time were fixed, respectively). IC₅₀ values were calculated as $0.6932/K_r$ and $t_{1/2}$ as $0.6932/K_c$. F_{min} was set to zero, as both pCMB and pCMBS completely inhibited transport. In Fig. 3C, a nonlinear regression fit to a one-site binding (hyperbola) curve determined the IC₅₀ values.

RESULTS

We have started a systematic approach (15) to the study of the structure-function relationships of the light subunits of the HAT family. The xCT light subunit was chosen as a model because of (i) its high activity in the oocyte expression system (5, 6); (ii) its narrow substrate selectivity (*i.e.* glutamate and cystine); and (iii) its sensitivity to organic mercurials (as shown by preliminary experiments; see below and Fig. 1).

The 4F2hc-xCT Heterodimer Is Inactivated by Mercurial Reagents—We tested the ability of pCMB and its impermeant derivative pCMBS to modify the transport elicited by the 4F2hc-xCT heterodimer in *Xenopus* oocytes. Both reagents completely inhibited glutamate transport in a dose-dependent manner with fast kinetics (at 1 min of incubation, the IC₅₀ values were $75.5 \pm 11.2 \mu\text{M}$ for pCMB and $300.4 \pm 89.7 \mu\text{M}$ for pCMBS; see also Figs. 3A and 4). The permeable reducing reagent β-mercaptoethanol completely reversed the inhibition when applied for 10 min at 5 mM, verifying that a cysteine(s) residue was the target of mercury compounds (data not shown). The impermeant reagent cysteine (10 mM for 10 min) also reversed the inhibition ($49.7 \pm 13.5\%$ of control value). The spontaneous reactivation was negligible for 10 min (data not shown).

Cys³²⁷ in Transmembrane Domain 8 Is the Main Target for pCMB and pCMBS Transport Inactivation—We next examined which subunit carried the targeted cysteine(s). 4F2hc has two cysteines, one (Cys¹⁰⁹) forming a disulfide bond with the xCT light subunit (Fig. 1). Early studies reported that 4F2hc cysteines are not essential for transport activity (16, 18). The expression of xCT together with 4F2hc without cysteines (Cysless 4F2hc) did not severely affect transport function (Fig. 1). pCMB and pCMBS fully inhibited glutamate transport, indicating that the target cysteine(s) was located in xCT. The seven endogenous cysteines of xCT (Fig. 2A) were mutated to serine in different combinations and transport activity, and pCMB/pCMBS reactivity was assayed. As shown in Fig. 2B, 100 μM L-glutamate uptake was relatively unaffected by the mutations, indicating that neither of the cysteines was essential *per se* for function. Strikingly, only C327S completely lost sensitivity to both pCMB and pCMBS, suggesting that this cysteine

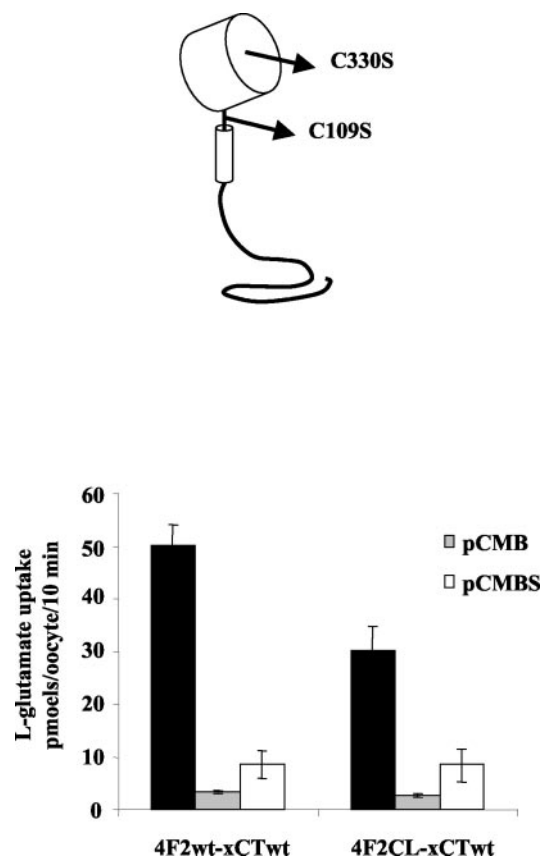


FIG. 1. The xCT light subunit of the 4F2hc-xCT heteromeric transporter confers sensitivity to the mercury compounds pCMB and pCMBS. Oocytes were injected with the xCT cRNA together with the 4F2hc wild type cRNA or Cysless 4F2hc (4F2CL). The top panel depicts the intracellular N terminus, the transmembrane domain (smaller cylinder), and the extracellular domain (larger cylinder) of 4F2hc with the location of the replaced cysteines. After 3 days the oocytes were preincubated with pCMB, pCMBS, or vehicle prior to assay L-glutamate uptake as stated under "Experimental Procedures." A representative experiment is shown.

was the main target of the reagents. The result was confirmed by generating a Cysless form of the xCT (Cysless xCT) and reintroducing Cys³²⁷ (Cysless-C327) in this background (Fig. 2C). The Cysless xCT was 10–20% active compared with the wild type (which is enough for functional studies, given the high transport activity of the wild type). As expected, Cysless-C327, but not Cysless, was sensitive to both pCMB and pCMBS. We concluded that Cys³²⁷ is the main target of pCMB and pCMBS.

Topology predictions for xCT with a variety of different computer algorithms locate Cys³²⁷ in the middle of transmembrane domain 8 (2, 5) (Fig. 2A). Results from our group using the 3-(*N*-maleimidylpropionyl)biocytin labeling procedure (19) show that the preceding loop is extracellular, whereas the next loop is intracellular.² Despite transmembrane localization, the sensitivity of Cys³²⁷ to the impermeant reagents pCMBS and cysteine indicate that it is accessible to the extracellular aqueous environment.

Cys³²⁷ Is Located in a Structurally Restricted Environment—The effect of other cysteine-specific reagents (MTS reagents, NEM, iodoacetamide, ([4-(*N*-maleimido)benzyl] trimethylammonium, and mersalyl acid; see "Experimental Procedures") was tested. At the concentrations used, none of them inhibited 4F2hc-xCT L-glutamate uptake even when this amino acid was present with the reagent during the preincubation time (data

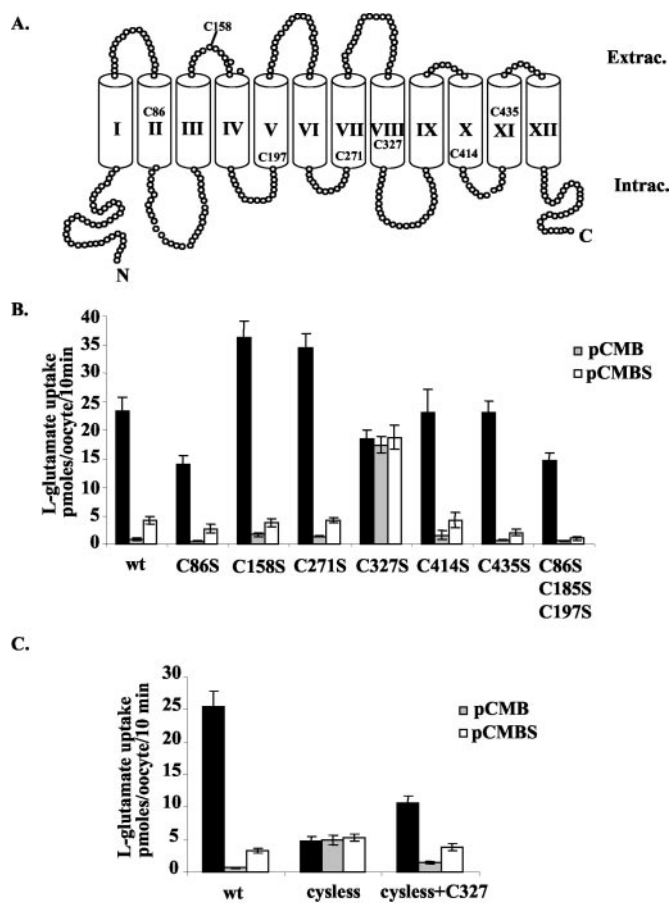


FIG. 2. The xCT residue Cys³²⁷ is the target for transport inactivation by pCMB and pCMBS. A, the predicted topological model for the xCT transporter. The protein has 12 transmembrane domains with intracellular N and C termini. Location of the seven endogenous cysteines is shown. B, different Cys to Ser substitutions were generated in a wild type xCT background. xCT cRNAs were injected together with 4F2hc cRNA. L-glutamate uptake was tested after preincubation with pCMB, pCMBS, or vehicle, as described in the legend to Fig. 1. A representative experiment is shown. The results from another independent experiment are similar. C, an xCT devoid of cysteines was constructed (Cysless), and Cys³²⁷ was re-introduced in this background (Cysless+C327). L-Glutamate transport in oocytes was assayed as described previously. A representative experiment is shown.

not shown). The same result was obtained with the Cysless-C327 xCT (data not shown). The reagents may have not reacted with any cysteine, or the reaction may have not affected transport activity. To distinguish between the two possibilities, oocytes expressing 4F2hc-xCT were preincubated with the different cysteine reagents, washed, and incubated again with pCMB under conditions that should normally lead to transport inhibition. The preincubation did not modify pCMB inhibition, indicating that they did not have access to Cys³²⁷ (data not shown). Given the diversity of the reagents used (in size, structure, reaction mechanism, and membrane permeability), pCMB and pCMBS may gain access to Cys³²⁷ via a structurally restricted pathway.

xCT Substrates Protect from Transport Inactivation—The above data indicate that Cys³²⁷ is accessible at least to the extracellular medium during the transport cycle. This raised the possibility that this residue may be part of (or close to) the substrate permeation pathway. If this is true, amino acid substrates should delay the reaction of pCMB and pCMBS. Indeed, glutamate (Fig. 3A) and cystine (data not shown) strongly protected 4F2hc-xCT L-glutamate uptake from pCMB and pCMBS inhibition. The calculated $t_{1/2}$ values were, for pCMB, 83.5 ± 7 s in the absence of amino acid, 1475 ± 690 s in the

² E. Gasol and M. Palacín, manuscript in preparation.

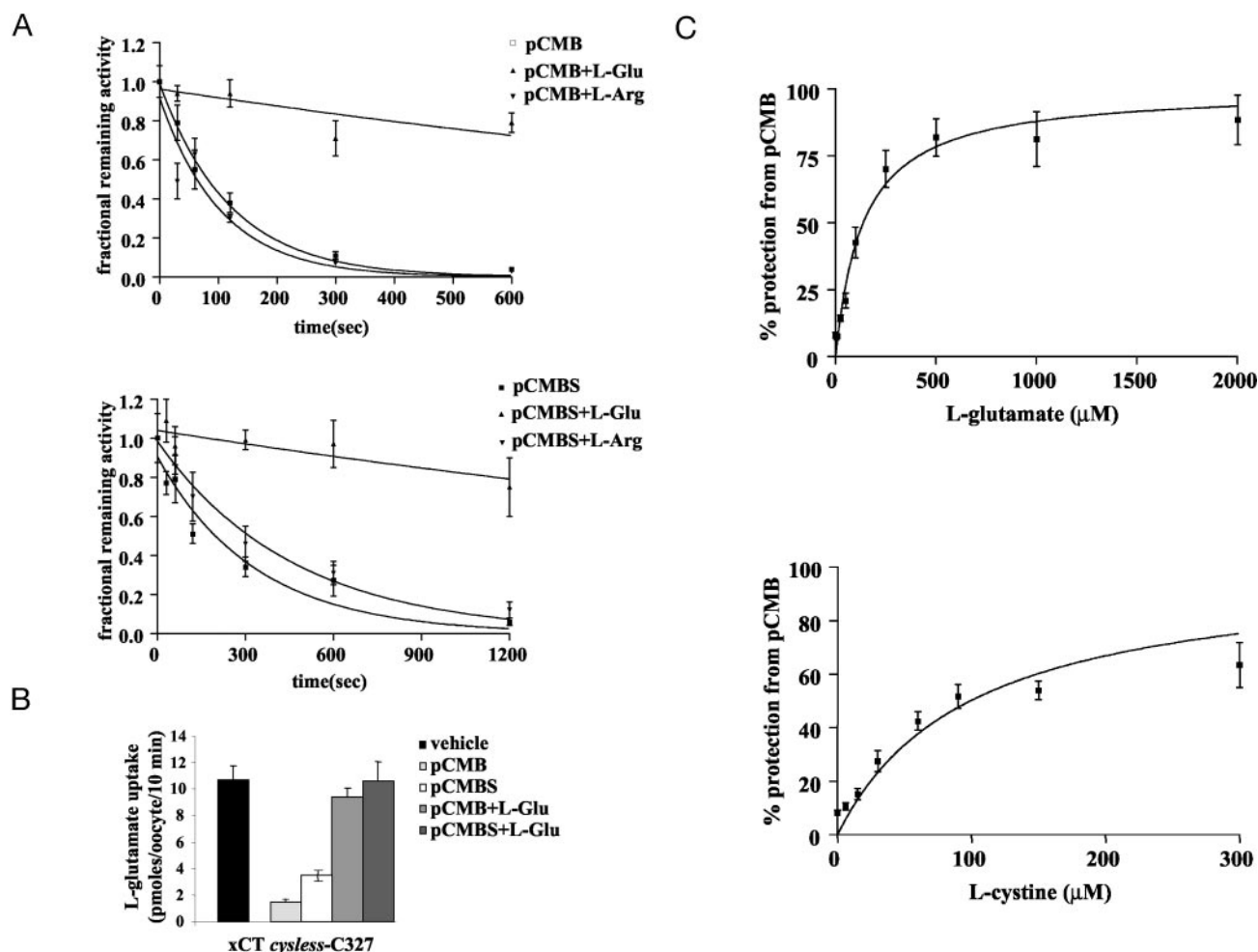


FIG. 3. **Substrate protection from pCMB and pCMBS-mediated transport inactivation.** **A**, time-dependent inactivation of L-glutamate transport measured in oocytes injected with 4F2hc and xCT cRNAs after the preincubation with either pCMB (top) or pCMBS (bottom) alone or in combination with L-glutamate or L-arginine. The results are expressed as the fractional remaining activity compared with the transport without prior preincubation. **B**, oocytes injected with 4F2hc and Cysless C327 xCT cRNAs were preincubated with the indicated reagents and washed, and L-glutamate uptake was assayed as described previously. **C**, oocytes injected with 4F2hc and xCT cRNAs were preincubated with vehicle or with pCMB, alone or together, with the indicated concentrations of either L-glutamate (top) or L-cystine (bottom), washed, and L-glutamate uptake was measured. L-Cystine concentration was not increased because of its poor solubility in the uptake medium. Results are expressed as the percentage of protection from pCMB-mediated transport inactivation compared with the control without amino acids. Representative experiments are shown.

presence of L-glutamate, and 72.5 ± 21.7 s in the presence of L-arginine; and for pCMBS, 230.7 ± 51.4 s in the absence of amino acid, 3081 ± 959 s in the presence of L-glutamate, and 319.4 ± 39 s in the presence of L-arginine. As expected, L-arginine, neither a substrate nor an inhibitor, did not protect. Similar results were obtained with the Cysless-C327 xCT (Fig. 3B). Moreover, half-maximal protection (Fig. 3C) occurred at substrate concentrations similar to the K_m measured in *Xenopus* oocytes (in the presence of pCMB, IC_{50} was 138 ± 16.3 μ M for L-glutamate and 99.2 ± 9.2 μ M for L-cystine) (see Refs. 5 and 6 and Table I), suggesting that substrate protection of the Cys³²⁷ residue occurs at a step within the transport process.

At least two different mechanisms may account for protection: (i) substrates may directly compete with pCMB and pCMBS for the substrate binding site/permeation pathway, or alternatively, (ii) a substrate-induced conformational change may occlude the access of mercury compounds to Cys³²⁷. It is generally accepted that large conformational changes in proteins are much more sensitive to temperature changes than substrate binding (20, 21). This feature has been exploited experimentally to detect conformational changes in different carriers such as the serotonin transporter (22) and the neuronal glycine transporter (23). We carried out a time course of the modification of xCT by pCMB (50 μ M) in the presence of glutamate (2 mM) at 25 and 4 °C (Fig. 4). pCMB completely inhibited uptake at both temperatures although, as expected, at a slower rate at 4 °C ($t_{1/2} = 63.6 \pm 9$ s at 25 °C and 436 ± 110 s at 4 °C). Glutamate equally protected from the inhibition both at 25 and 4 °C ($t_{1/2} = 1272 \pm 455$ s⁻¹ at 25 °C and 6932 ± 4852 s at 4 °C). Thus, glutamate protects the Cys³²⁷ residue at a step in the transport cycle, most likely prior to temperature-sensitive substrate-induced conformational changes.

TABLE I

Kinetic parameters of Cys³²⁷ mutants

Oocytes were injected with 4F2hc cRNA together with cRNA from the wild type xCT or Cys³²⁷ mutations to serine, alanine, leucine, or threonine. After 3 days, transport of 5 - 2000 μ M L-[³H]glutamate was measured and kinetic parameters determined. Values represent the means \pm S.E. of $n = 2-4$ determinations. ND, not determined.

	K_m	V_{max}
	μ M	pmol/oocyte/10 min
Wt	173.7 ± 15.3	131.4 ± 9
C327S	359.8 ± 62^a	125.6 ± 7.2
C327A	267.6 ± 19.9^a	112.8 ± 2.6
C327L	ND	ND
C327T	186.3 ± 31.2	71.3 ± 3.4

^a Statistically significant (*F* test, $p < 0.005$) compared with the wild type.

mate (2 mM) at 25 and 4 °C (Fig. 4). pCMB completely inhibited uptake at both temperatures although, as expected, at a slower rate at 4 °C ($t_{1/2} = 63.6 \pm 9$ s at 25 °C and 436 ± 110 s at 4 °C). Glutamate equally protected from the inhibition both at 25 and 4 °C ($t_{1/2} = 1272 \pm 455$ s⁻¹ at 25 °C and 6932 ± 4852 s at 4 °C). Thus, glutamate protects the Cys³²⁷ residue at a step in the transport cycle, most likely prior to temperature-sensitive substrate-induced conformational changes.

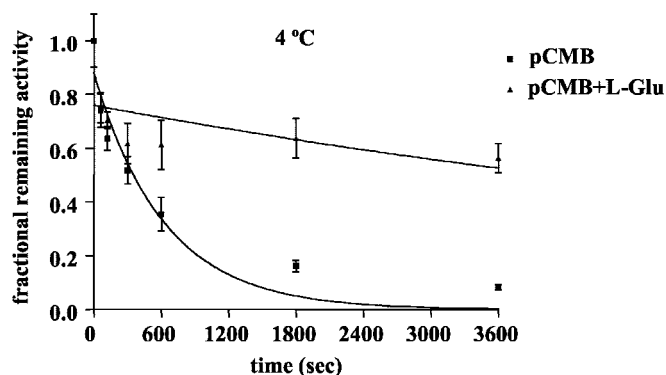
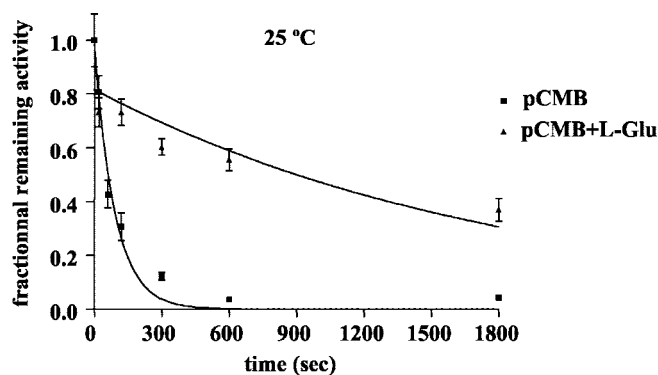


FIG. 4. **Temperature dependence of substrate protection.** The experiment described in Fig. 3A legend was repeated at 25 °C (*top*) and 4 °C (*bottom*). In the latter case, preincubations were made at 4 °C, and subsequent washes and transport assay were done at 25 °C. Note the different time scales in both panels because of the slower reactivity of pCMB at 4 °C. A representative experiment is shown. Similar data was obtained in two other experiments with different oocyte batches.

Analysis of Cys³²⁷ Mutants—Cys³²⁷ residue is either conserved or changed to Thr in the known mammalian LSHAT sequences (see Fig. 5A). Therefore, it is not expected to be a determinant of substrate specificity. Nevertheless, our results are consistent with a role for this residue in substrate binding. To test this hypothesis, we mutated Cys³²⁷ to Ser, Ala, Thr, and Leu and measured the transport function and expression (Figs. 5B and 6, and Table I). No significant differences were found between wild type and C327S, C327A, and C327T when 100 μ M L-glutamate uptake was assayed. However, we observed a clear tendency of L-glutamate transport to decrease in the C327S mutant ($72.5 \pm 6\%$ compared with the wild type) (Fig. 5B). The C327L mutant was inactive (Fig. 5B) even when 10 mM glutamate uptake was assayed (data not shown). Kinetic analysis revealed a slight increase in the K_m for glutamate in the Ser and Ala mutants (2- and 1.5-fold, respectively) (Table I), which was statistically significant (*F*-test, $p < 0.005$). Cysless xCT showed a 1.9-fold increase in the K_m for glutamate ($328.8 \pm 66.2 \mu$ M) compared with wild type (Table I). Interestingly, re-introducing the Cys³²⁷ in the Cysless xCT background decreased by 2.6-fold the K_m for glutamate ($124.1 \pm 23 \mu$ M), resembling the K_m for glutamate in wild type xCT (Table I). Thus, mutation of Cys³²⁷ to Ser produces a similar increase in the K_m for glutamate in the wild type and Cysless backgrounds. Moreover, the pH dependence of the xCT-mediated cystine transport (6) was not modified when Cys³²⁷ was re-introduced in the Cysless background ($K_{0.5}$ values were 7 ± 0.20 and 6.7 ± 0.25 for Cysless xCT and xCT Cysless-C327, respectively). On

A.

	TM VIII
b ⁰ -AT	VLYPASWIVPLFVAFSTIGAANGTCFTAG
y+LAT1	IFGIFNWIIPLSVALSCFGGLNASIVAAS
y+LAT2	TFGMFSWTIPIAVALSCFGGLNASIFASS
LAT1	HLGVMSWIIIPVGVGLSCFGSVNGSLFTSS
LAT2	LLGVMAWIMPIVALSTFGGVNGSLFTSS
xCT	LLGNFSLAVPIFVALSCFGSMNGGVFAVS
asc1	LLGYFSWVMPVSVALSTFGGINGYLFTYS

↑

B.

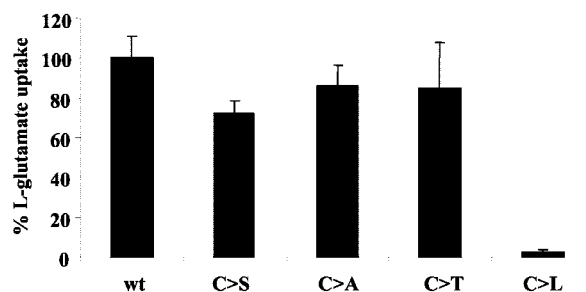


FIG. 5. **Transport activity of Cys³²⁷ mutants.** A, LSHAT alignment of the transmembrane (TM) domain VIII (*underlined*) (only the human proteins are shown). The residue corresponding to xCT Cys³²⁷ is *bolded*. ClustalW software was used for the alignment, and the HMMTOP algorithm was used for transmembrane domain assignment. Although the limits of the transmembrane domains slightly vary between different algorithms, Cys³²⁷ is always located in the middle of transmembrane domain VIII, somehow biased to the C-terminal half. B, oocytes were injected with 4F2hc cRNA and the different Cys³²⁷ mutant cRNAs. After 3 days 100 μ M L-glutamate uptake was measured. The values represent the means \pm S.E. of 3–5 determinations. No significant differences were found between groups (except for the C327L mutant).

the other hand, there was a tendency to shift the $K_{0.5}$ to more basic values when compared with the wild type ($K_{0.5}$ was 6.3 ± 0.25), suggesting that other cysteines (but not Cys³²⁷) might have a role in the pH dependence.

To check for transporter expression, Myc-tagged wild type and mutant xCT transporters were constructed. Their activity and sensitivity toward pCMB and pCMBs were indistinguishable from the untagged versions (Fig. 6A and data not shown). All xCT variants (in the presence of 4F2hc) were expressed at similar levels on the oocyte surface as judged by immunofluorescence experiments (Fig. 6B). Therefore, large changes in transporter expression at the plasma membrane do not account for the functional differences among the Cys³²⁷ variants. More important, the inactive phenotype of the C327L xCT is not due to folding/trafficking alterations and may reflect a defective transport cycle. Together, the results suggest a location of Cys³²⁷ close to the substrate binding site.

DISCUSSION

Here we provide evidence suggesting that Cys³²⁷ is located close to the substrate permeation pathway of xCT. When mutated, residues involved in the binding of substrates are expected to modify the K_m and the substrate selectivity (24, 25). Cys³²⁷ is either a cysteine or a threonine in the mammalian

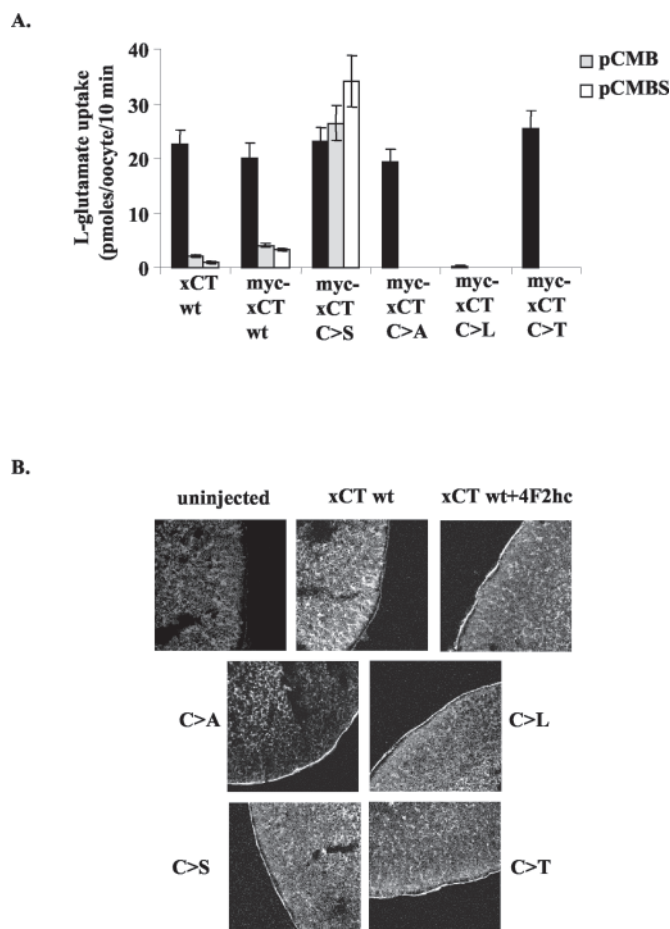


FIG. 6. Transport activity, mercury compounds sensitivity, and localization of Myc-tagged wild type (*wt*) xCT and Cys³²⁷ mutants. A, oocytes were injected with 4F2hc cRNA and the indicated xCT cRNAs. After 3 days, L-glutamate uptake (100 μ M) was measured. Sensitivity to pCMB and pCMBS was tested as described in Fig. 2B legend. A representative experiment is shown. B, oocytes expressing xCT alone (*xCT wt*), together with 4F2hc (+4F2hc), the Cys³²⁷ mutants (C>A,L,S,T) together with 4F2hc, or uninjected were subjected to immunofluorescence experiments (see “Experimental Procedures”) with the anti-Myc-specific antibody (all xCT versions were Myc-tagged). Two different batches of oocytes gave similar results.

LSHAT proteins (Fig. 5A). No correlation is found with substrate selectivity of the different transporters; as an example, y⁺LAT1 and -2, LAT1, and xCT light subunits transport basic and neutral amino acids, large neutral amino acids, and acidic amino acids, respectively (1, 2). Therefore, variations in substrate selectivity are not expected in the Cys³²⁷ xCT mutants. In this sense, neither transport of L-arginine nor L-leucine was detected in the C327S xCT mutant (data not shown). On the other hand, we observed a higher K_m in the C327S and C327A mutants but not in the C327T mutant (Table I). Threonine is the residue found in this position in some LSHAT proteins (see Fig. 5A). Although low (1.5–2-fold), the increase in K_m is in the range of those found in other studies; Cys¹⁴⁴ of the creatine transporter (CreaT) is located close to the substrate binding site, and a C144A mutant displays a 1.7-fold higher K_m (24); on the well studied lactose permease (LacY) Cys¹⁴⁸ mutants (to Ala, Ser, Thr, and Val) either decrease or increase the K_m for lactose from 1.5 to 2.6-fold (25). Analyses of the Cys³²⁷ mutants show that a small side chain is required at this position and bulky amino acids are not tolerated (C327L mutant; see Figs. 5B and 6), indicating that this residue, if not essential, is at least important for the transport cycle. Preliminary results show that size restrictions may be even more important in

other LSHAT proteins; mutation of the homologous cysteine to serine in y⁺LAT1 abolishes transport (data not shown). Therefore, we favor a scenario in which Cys³²⁷ could be close to the xCT substrate binding site; small side chains at this position are permissive for substrate binding and/or translocation, although they do not bind substrate, and bulky amino acids may impose a strong steric restriction to the transport cycle. Although structurally unrelated to xCT, it is interesting to note that the recently reported crystal structure of LacY (26) indicates that the K_m effects of Cys¹⁴⁸ mutants (see above) are explained by steric hindrance of the substrate binding site.

Independent support for a link of the Cys³²⁷ residue to the permeation pathway comes from our studies with pCMB and pCMBS. First, Cys³²⁷-dependent transport inactivation by pCMB and pCMBS is protected by substrates with an IC₅₀ similar to the K_m (Fig. 3). This protection is temperature-independent, suggesting that no large conformational changes are involved (20, 21). We do not exclude the possibility, however, that minor conformational changes were not detected by the temperature dependence experiment. Second, despite its location in the middle of transmembrane domain 8, Cys³²⁷ is targeted by the impermeant reagents pCMBS and cysteine, indicating that it is accessible to the aqueous environment (Fig. 2). Cys³²⁷ may be facing the extracellular medium, as pCMB, pCMBS, and cysteine were unable to react with this residue when injected into the oocytes at a high millimolar final concentration (data not shown). Spontaneous reactivation of the pCMB or pCMBS inactivation was not observed but may occur at an extremely slow rate. However, these data must be interpreted with caution (27); the sulfhydryl reagents may be quenched by a large excess of thiols in the oocyte cytosol, and intracellular cysteine may be rapidly incorporated to glutathione. Moreover, as xCT mediates cystine/glutamate antiport, intracellular binding sites may be saturated by the large concentration of L-glutamate in oocytes (28), preventing access of the reagents to Cys³²⁷.

A striking feature of Cys³²⁷ is its inaccessibility to a variety of other thiol-reactive compounds. A similar reaction pattern has been described for the V165C mutation in GLUT1 (glucose transporter-1 (27)) and for Cys³⁰⁰ in GABP (*Escherichia coli* γ -aminobutyric acid permease (29)). In both cases a similar size and shape of the aromatic ring of pCMB and pCMBS and substrates of those transporters were invoked to explain the rapid access of these reagents compared with some MTS reagents (29), iodoacetate, and NEM (27, 29). This can hardly apply to the xCT transporter, and as expected, millimolar concentrations of pCMB or pCMBS did not inhibit transport when assayed on the C327S mutant (data not shown). The specific effect of pCMB and pCMBS may be related to the stacking of the aromatic ring with vicinal Phe or Tyr residues; there are three Phe residues in transmembrane domain 8 (Phe³¹⁵, Phe³²², and Phe³²⁸, see Figs. 5A and 7).

Amino acid residues surrounding Cys³²⁷ in transmembrane domain 8 lie on a highly conserved region in the LSHAT family (Figs. 5 and 7), and therefore they are not expected to play a major role in substrate selectivity. However, this region might be important for some general transport step(s). A preliminary model of the amino acid binding site has recently been proposed for the LSHATs LAT1 and y⁺LAT1 (11, 12). The authors suggest three recognition subsites: one for the α -carboxyl group, one for the α -amino group, and one for the side chains. Whereas the latter would be divergent in each member of the family, the first two may be similar or conserved among all the members. Cys³²⁷ might be part of these subsites.

To gain more insight into the functional role of Cys³²⁷, we closely inspected the region including transmembrane domain

	I II
xCT	FSLAVPIFVAL SC FGSMNGGVFAVSRLFYVASREGHLPEI
LAT1	MSWIIPV FVGL SC FGSVNGSLFTSSRLFFVGSREGHLPSI
LAT2	MAWIMPISVAL ST FGGVNGSLFTSSRLFFAGAREGHLPSV
y ⁺ LAT1	FNWIIPLSV ALSC FGGLNASIVAASRLFFVGSREGHLPSI
y ⁺ LAT2	FSWTIPIAVAL SC FGGLNASIFASSRLFFVGSREGHLPSI
asc1	FSWVMPVSVAL ST FGGINGYLFYTSRLCFSGAREGHLPSL
b ^{0,+} AT	ASWIVPLFVAF ST IGAANGTCFTAGRLIYVAGREGHMLKV
cadB	AAPLVSAFTA FA CLTSLGSWMMLVGQAGVRAANDGNFPKV
yjdB	AGAIVSFCAA AG CLGSLGGWTLTAGQTAKAAADDGLFPPI
potE_ECOLI	VGKVMALMVM SC CGSLLGWQFTIAQVFKSSSDEGYFPKI
potE_HAEIN	VGKVMGLMVM SC FGSLLGWQFTIAQVFKSSAEEGYPPAF
arcD	GAVLISVGLLI SLL GALLS WVLLCAEIMFAAAK DHTMPEF
lysI	GAALISLGLCL SVL GAYVSWQMLCAEPLAL MAMDGLIPSK
	: : . . .
gabP	AKLIMDCVILLSVT S CLNSALYTASRMLYSLSRRGDAPAV
	: : . . .

FIG. 7. Transmembrane domain 8 region in three different APC subfamilies. A ClustalW alignment was performed with the LSHAT mammalian proteins (only the human orthologues are shown) (subfamily 2.A.3.8), the APA proteins (subfamily 2.A.3.2), and gabP from *E. coli*, a member of the 2.A.3.1 subfamily. The dots (period and colon) indicate conserved residues. The predicted transmembrane domain VIII was found with the HMMTOP algorithm. The eight residues from the two overlapping (G/S/A)XXX(G/S/A) motifs (I and II) are shown in bold. Note that only motif II is conserved in gabP. PCMB- and pCMB-sensitive cysteines in both human xCT and in gabP proteins are shown as white letters within black squares. Residues within white squares have been shown to be important for transport activity. The residues in xCT very close to or within the transmembrane domain are shown in gray; the conserved Phe residue in LSHAT proteins is also in gray (it is substituted by Ile only in b^{0,+}AT). See "Discussion" for details. GenBankTM accession numbers for human LSHATs are: xCT, AB026891; LAT1, AF077866; LAT2, AF171669; y⁺LAT1, AF092032; y⁺LAT2, D87432; asc1, NM_019849; b^{0,+}AT, AF141289. GenBankTM accession numbers for the APA proteins are: *E. coli* cadB, AAP76293; *E. coli* yjdB, P39269; *E. coli* potE, NP_415219; *Haemophilus influenzae* potE, P44768; *Pseudomonas aeruginosa* arcD, P18275; *Corynebacterium glutamicum* lysI, CAA42855; *E. coli* gabP, NP_31551.

8 and compared it with related transport proteins. The LSHAT proteins belong to the 2.A.3.8 family of APC (amino acid/polyamine/organic cation) transporters (30). Within the APC superfamily, the LSHATs can be aligned along the whole sequence, despite the low identity (14–16%), with the prokaryotic transporter proteins PotE, YjdB, CadB, and LysI (2.A.3.2 family or APA (basic amino acid/polyamine antiporters)) (30). The alignment over transmembrane domain 8 and part of intracellular loop 4 of these proteins with the human LSHATs (including xCT) interacting with 4F2hc or rBAT is shown in Fig. 7. Two overlapping (G/S/A)X₁X₂X₃(G/S/A) motifs (see Fig. 7, motifs I and II) are found, which have been reported to constitute a framework for transmembrane helix-helix association (31, 32). X represents any amino acid. It is possible that in the xCT context a bulky side chain like Leu in the X₁ of motif I may cause alterations in helix packing leading to transport inactivation. In PotE, three important residues for transport are located in this transmembrane domain; one of them is the cysteine at the same position of the alignment (33). Interestingly, Cys³⁰⁰ in the GABP protein (see above) is also located in transmembrane domain 8, and is the X₁ of a (G/S/A)X₁X₂X₃(G/S/A) motif; it corresponds to motif II in the alignment among LSHATs and the proteins from family 2.A.3.2 (Fig. 7), and it seems to be conserved among proteins from the 2.A.3.1 AAT family (amino acid transporter) to which GABP belongs and the 2.A.3.10 YAT family (yeast amino acid transporter) (34). Cys³⁰⁰ in GABP is targeted by sulfhydryl reagents in a manner similar to xCT Cys³²⁷ (29). Mutation to Ala renders a protein 5% active compared with the wild type. Although the mutant retains substrate binding, no comparison with the wild type protein was made, and therefore its role in substrate binding is unclear

(35). The GABP Cys³⁰⁰ seems to initiate a 20-amino acid residue amphipathic α -helix comprising the C-terminal half of transmembrane domain 8 and extending into the fourth intracellular loop connecting TM8 and TM9. The authors have speculated that this structure may be conserved among the members of the 2.A.3.1 and 2.A.3.10 families (29, 34, 35, 36). Further studies are needed to address whether a similar structure may exist in other APC families (*i.e.* LSHAT family, APA family, etc). Indeed, there is evidence indicating an important function for this region; the type B cystinuria mutation, R333W, and the lysinuric protein intolerance mutation, L334R, impair transport (human b^{0,+}AT and human y⁺LAT1, respectively) and lie on intracellular loop 4 (14, 37). On the CAT (cationic amino acid) transporters (the 2.A.3.3 family of APC), this loop modulates substrate affinity (38, 39).

We have therefore identified Cys³²⁷ of xCT as the target of inactivation by mercurial reagents. Substrate protection experiments and analysis of Cys³²⁷ mutants favor a view in which this residue lies close to the substrate binding site. Our data are still compatible with slight conformational changes occurring upon substrate binding, together with a partial overlap between substrate and pCMB/pCMB binding sites. A non-transported substrate analogue (21), not yet available for the 4F2hc-xCT transporter, would be useful in distinguishing these possibilities. To our knowledge, this is the first systematic effort to elucidate the structure-function relationships in the LSHAT family. The Cys³²⁷ active mutants and the Cysless xCT protein will provide an excellent background for probing residues in transmembrane domain 8 and other domains by cysteine-scanning mutagenesis.

Acknowledgments—We thank Dr. Marta Camps for help and advice with the immunofluorescence experiments, Dr. Josep Lluís Gelpi for help with data analysis, Judit García for technical assistance, and Robin Rycroft for editorial support.

REFERENCES

- Verrey, F., Meier, C., Rossier, G., and Kuhn, L. C. (2000) *Pflugers Arch. Eur. J. Physiol.* **440**, 503–512
- Chillaron, J., Roca, R., Valencia, A., Zorzano, A., and Palacin, M. (2001) *Am. J. Physiol.* **281**, F995–F1018
- Nakamura, E., Sato, M., Yang, H., Miyagawa, F., Harasaki, M., Tomita, K., Matsuoka, S., Noma, A., Iwai, K., and Minato, N. (1999) *J. Biol. Chem.* **274**, 3009–3016
- Reig, N., Chillaron, J., Bartocioni, P., Fernandez, E., Bendahan, A., Zorzano, A., Kanner, B., Palacin, M., and Bertran, J. (2002) *EMBO J.* **21**, 4906–4914
- Sato, H., Tamba, M., Ishii, T., and Bannai, S. (1999) *J. Biol. Chem.* **274**, 11455–11458
- Bassi, M. T., Gasol, E., Manzoni, M., Pineda, M., Riboni, M., Martin, R., Zorzano, A., Borsani, G., and Palacin, M. (2001) *Pflugers Arch. Eur. J. Physiol.* **442**, 286–296
- Sato, H., Tamba, M., Okuno, S., Sato, K., Keino-Masu, K., Masu, M., and Bannai, S. (2002) *J. Neurosci.* **22**, 8028–8033
- Bannai, S., Sato, H., Ishii, T., and Sugita, Y. (1989) *J. Biol. Chem.* **264**, 18480–18484
- Sato, H., Kuriyama-Matsumura, K., Hashimoto, T., Sasaki, H., Wang, H., Ishii, T., Mann, G. E., and Bannai, S. (2001) *J. Biol. Chem.* **276**, 10407–10412
- Sasaki, H., Sato, H., Kuriyama-Matsumura, K., Sato, K., Maehara, K., Wang, H., Tamba, M., Itoh, K., Yamamoto, M., and Bannai, S. (2002) *J. Biol. Chem.* **277**, 44765–44771
- Uchino, H., Kanai, Y., Kim do, K., Wempe, M. F., Chairoungdua, A., Morimoto, E., Anders, M. W., and Endou, H. (2002) *Mol. Pharmacol.* **61**, 729–737
- Kanai, Y., and Endou, H. (2001) *Curr. Drug Metab.* **2**, 339–354
- Boado, R. J., Li, J. Y., and Pardridge, W. M. (2003) *J. Neurochem.* **84**, 1322–1331
- Mykkanen, J., Torrents, D., Pineda, M., Camps, M., Yoldi, M. E., Horelli-Kuitunen, N., Huoponen, K., Heinonen, M., Oksanen, J., Simell, O., Savontaus, M. L., Zorzano, A., Palacin, M., and Aula, P. (2000) *Hum. Mol. Genet.* **9**, 431–438
- Kaback, H. R., Sahin-Toth, M., and Weinglass, A. B. (2001) *Nat. Rev. Mol. Cell Biol.* **2**, 610–620
- Estevez, R., Camps, M., Rojas, A. M., Testar, X., Deves, R., Hediger, M. A., Zorzano, A., and Palacin, M. (1998) *FASEB J.* **12**, 1319–1329
- Bertran, J., Werner, A., Moore, M. L., Stange, G., Markovich, D., Biber, J., Testar, X., Zorzano, A., Palacin, M., and Murer, H. (1992) *Proc. Natl. Acad. Sci. U. S. A.* **89**, 5601–5605
- Pfeiffer, R., Spindler, B., Loffing, J., Skelly, P. J., Shoemaker, C. B., and Verrey, F. (1998) *FEBS Lett.* **439**, 157–162
- Grunewald, M., Bendahan, A., and Kanner, B. I. (1998) *Neuron* **21**, 623–632
- Chen, J. G., and Rudnick, G. (2000) *Proc. Natl. Acad. Sci. U. S. A.* **97**, 1044–1049
- Seal, R. P., and Amara, S. G. (1998) *Neuron* **21**, 1487–1498
- Androutsellis-Theotokis, A., Ghassemi, F., and Rudnick, G. (2001) *J. Biol. Chem.* **276**, 45933–45938
- López-Corcuera, B., Núñez, E., Martínez-Maza, R., Geerlings, A., and Aragón, C. (2001) *J. Biol. Chem.* **276**, 43463–43470
- Dodd, J. R., and Christie, D. L. (2001) *J. Biol. Chem.* **276**, 46983–46988
- Jung, H., Jung, K., and Kaback, H. R. (1994) *Biochemistry* **33**, 12160–12165
- Abramson, J., Smirnova, I., Kasho, V., Verner, G., Kaback, H. R., and Iwata, S. (2003) *Science* **301**, 611–615
- Mueckler, M., and Makepeace, C. (1997) *J. Biol. Chem.* **272**, 30141–30146
- Meier, C., Ristic, Z., Klauser, S., and Verrey, F. (2002) *EMBO J.* **21**, 80–89
- Hu, L. A., and King, S. C. (1999) *Biochem. J.* **339**, 649–655
- Jack, D. L., Paulsen, I. T., and Saier, M. H. (2000) *Microbiology* **146**, 1797–1814
- Russ, W. P., and Engelman, D. M. (2000) *J. Mol. Biol.* **296**, 911–919
- Senes, A., Gerstein, M., and Engelman, D. M. (2000) *J. Mol. Biol.* **296**, 921–936
- Kashiwagi, K., Kuraishi, A., Tomitori, H., Igarashi, A., Nishimura, K., Shirahata, A., and Igarashi, K. (2000) *J. Biol. Chem.* **275**, 36007–36012
- Hu, L. A., and King, S. C. (1998) *Biochem. J.* **330**, 771–776
- Hu, L. A., and King, S. C. (1998) *J. Biol. Chem.* **273**, 20162–20167
- Hu, L. A., and King, S. C. (1998) *Biochem. J.* **336**, 69–76
- Font, M. A., Feliúbadalo, L., Estivill, X., Nunes, V., Golomb, E., Kreiss, Y., Pras, E., Bisceglia, L., d'Adamo, A. P., Zelante, L., Gasparini, P., Bassi, M. T., George, A. L., Jr., Manzoni, M., Riboni, M., Ballabio, A., Borsani, G., Reig, N., Fernandez, E., Zorzano, A., Bertran, J., Palacin, M., and International Cystinuria Consortium (2001) *Hum. Mol. Genet.* **10**, 305–316
- Closs, E. I., Lyons, C. R., Kelly, C., and Cunningham, J. M. (1993) *J. Biol. Chem.* **268**, 20796–20800
- Habermeier, A., Wolf, S., Martine, U., Graf, P., and Closs, E. I. (2003) *J. Biol. Chem.* **278**, 19492–19499